PROCEEDINGS B

royalsocietypublishing.org/journal/rspb

Research

Cite this article: Parvizi E, Fraser CI, Dutoit L, Craw D, Waters JM. 2020 The genomic footprint of coastal earthquake uplift. *Proc. R. Soc. B* **287**: 20200712. http://dx.doi.org/10.1098/rspb.2020.0712

Received: 30 March 2020
Accepted: 11 June 2020

Subject Category:
Evolution

Subject Areas:
evolution, environmental science

Keywords:
disturbance, *Durvillaea*, evolution, extreme events, marine phylogeography, population genomics

Author for correspondence:
Elahe Parvizi
e-mail: ellie.parvizi@gmail.com

Electronic supplementary material is available online at https://doi.org/10.6084/m9.figshare.c.5036324.

THE ROYAL SOCIETY PUBLISHING

The genomic footprint of coastal earthquake uplift

Elahe Parvizi[1], Ceridwen I. Fraser[2], Ludovic Dutoit[1,2], Dave Craw[3] and Jonathan M. Waters[1]

[1]Department of Zoology, [2]Department of Marine Science, and [3]Department of Geology, University of Otago, PO Box 56, Dunedin 9054, New Zealand

EP, 0000-0002-1695-8817; CIF, 0000-0002-6918-8959; JMW, 0000-0002-1514-7916

Theory suggests that catastrophic earth-history events can drive rapid biological evolution, but empirical evidence for such processes is scarce. Destructive geological events such as earthquakes can represent large-scale natural experiments for inferring such evolutionary processes. We capitalized on a major prehistoric (800 yr BP) geological uplift event affecting a southern New Zealand coastline to test for the lasting genomic impacts of disturbance. Genome-wide analyses of three co-distributed keystone kelp taxa revealed that post-earthquake recolonization drove the evolution of novel, large-scale intertidal spatial genetic 'sectors' which are tightly linked to geological fault boundaries. Demographic simulations confirmed that, following widespread extirpation, parallel expansions into newly vacant habitats rapidly restructured genome-wide diversity. Interspecific differences in recolonization mode and tempo reflect differing ecological constraints relating to habitat choice and dispersal capacity among taxa. This study highlights the rapid and enduring evolutionary effects of catastrophic ecosystem disturbance and reveals the key role of range expansion in reshaping spatial genetic patterns.

1. Introduction

Major environmental disturbances can drive widespread biological range shifts [1,2], and in the face of rapid contemporary environmental change, understanding how species-range dynamics shape biodiversity patterns is increasingly important [3]. In theory, such range shifts could dramatically restructure spatial biodiversity [4–7], even in the absence of selective processes and barriers to gene flow [4,5,8]. Although natural selection often plays a key role in structuring biodiversity (e.g. [9]), recent modelling studies suggest neutral processes [10] can also influence such patterns [4,8,11,12]. In particular, theoretical and laboratory experimental data suggest colonization processes such as priority effects often underpin the distribution of diversity, with first-arriving lineages having an advantage over latecomers [13–16]. Major disturbances are thought to generate broad-scale structuring of biodiversity over deep time scales [1], but compelling evidence of this phenomenon from natural populations over ecologically relevant time frames remains elusive.

To date, few studies have assessed the impacts of disruptive geological processes such as earthquakes, tsunamis and volcanic eruptions on biodiversity patterns [17–19]. Sudden coastal uplift [19–21] provides an unparalleled opportunity to elucidate the role of disturbance in structuring biodiversity. Intertidal habitats present elegant, essentially linear systems with which to test for impacts of earthquake-driven upheaval. Recent catastrophic earthquakes in New Zealand and Chile, for instance, raised extensive stretches of seabed by several metres, eliminating intertidal species and potentially creating widespread vacant intertidal habitats for colonization [21–24]. Evaluating the biological impacts of such events can enhance our understanding of the role of disturbance in shaping biodiversity.

Here, we focus on the biological effects of a prehistoric uplift event affecting Southern Ocean coastlines. The South Island of New Zealand is tectonically active with occasional large earthquakes affecting the eastern coast (figure 1*a*), as at Christchurch in 2011 and Kaikoura in 2016 (figure 1*b*). A large prehistoric earthquake approximately 800 years ago raised a substantial stretch of southern

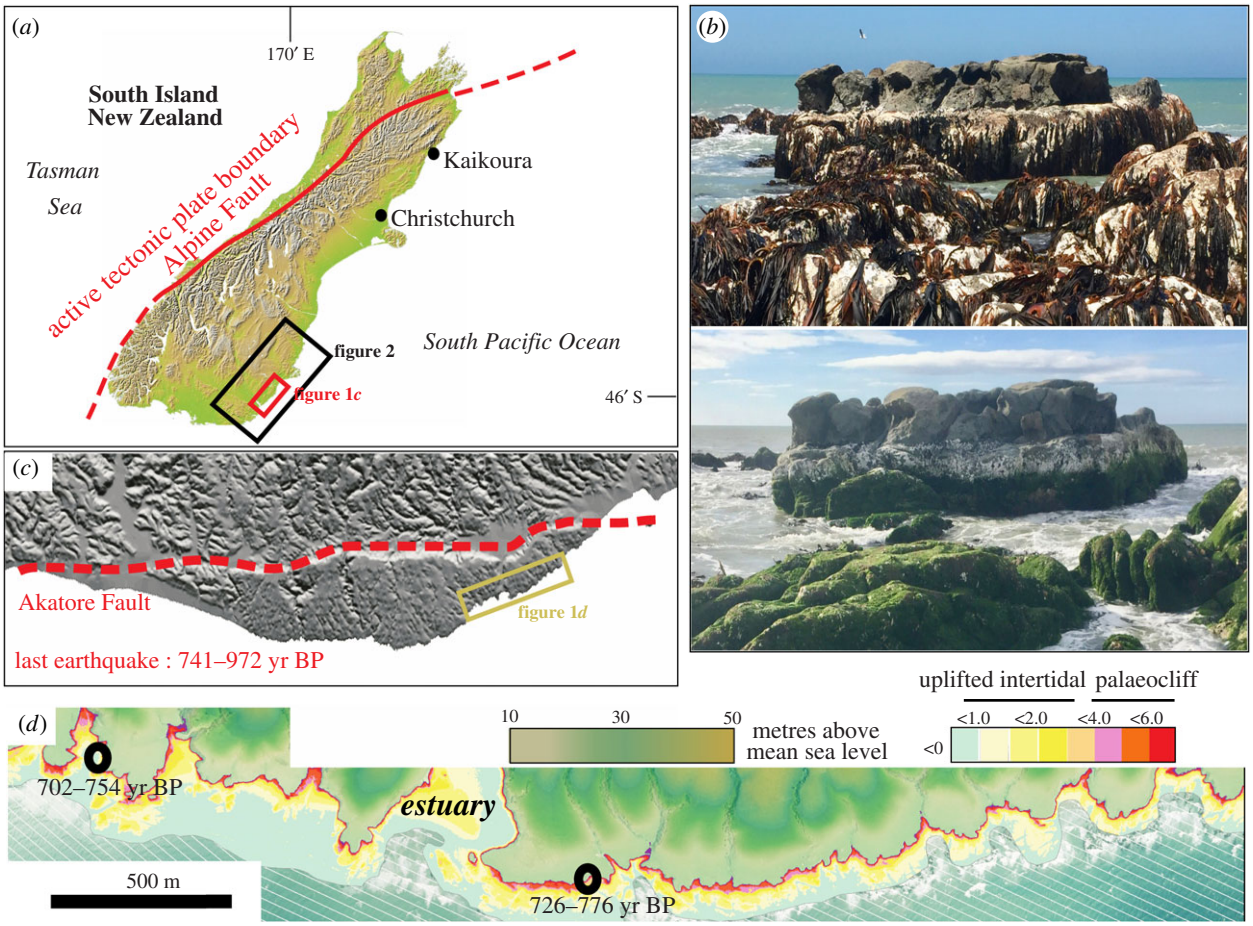

Figure 1. Major earthquake uplift events on Southern Ocean coastlines have extirpated intertidal biota. (*a*) Regional tectonic setting in South Island, New Zealand (*b*) A recent example of the effect of coastal uplift on intertidal kelps, in which habitat-forming *Durvillaea* kelp populations suffered widespread extirpation. Photos: J.M.W., Ward Beach (Kaikoura region; November 2016 and April 2017). (*c*) Topography of the Akatore coastal block uplifted by an earthquake approximately 800 years ago. (*d*) Colour-contoured LIDAR topography of a portion of uplifted coastline, showing uplifted intertidal zone in shades of yellow. Numbers on LIDAR map represent radiocarbon dates on uplifted shells in caves at palaeo-high tide. (Online version in colour.)

coastline by 2–3 metres [25–27] (figure 1*c*,*d*). The whole stretch of coast was affected by an approximately 800 yr BP event [26] dated by radiocarbon methods at the fault line itself [27] (figure 1*c*). Radiocarbon dating of shells at the palaeo-high-tide level (figure 1*d*) overlap the younger end of this radiocarbon date range and confirm the direct relationship between earthquake and coastal uplift.

We analysed single nucleotide polymorphism (SNP) data distributed across the genome of three sympatric bull-kelp species inhabiting rocky shores of southern New Zealand to test for lasting genomic signatures of this prehistoric coastal uplift. The three species differ in their dispersal capacities and tidal ranges [28] and thus in their vulnerabilities to extirpation by uplift. Specifically, *Durvillaea willana* is a non-buoyant shallow subtidal (to approximately 6 m) taxon, whereas *Durvillaea antarctica* is buoyant and dominates the low-intertidal, and *Durvillaea poha* is similarly buoyant but occupying more wave-sheltered habitats of the low-mid intertidal [28]. Our study reveals that environmental disturbance and colonization processes can rapidly reshape intraspecific spatial genetic patterns.

2. Results

(a) Earthquake-driven genetic structure

De novo assembly of loci yielded a total of 9526 SNPs in 113 individuals of *D. poha*, 9710 SNPs in 128 *D. antarctica* and 7384 SNPs in 73 *D. willana*. Phylogeographic analyses revealed distinctive spatial genomic sectors in both buoyant intertidal species (*D. antarctica* and *D. poha*), tightly linked to earthquake uplift boundaries. By contrast, no uplift-associated structure was detected in the less-dispersive, subtidal species, *D. willana* (figure 2).

For both intertidal species, principal component analysis (PCA), STRUCTURE and BAPS clustering methods all detected abrupt shifts in genotype compositions associated with the uplift zone, tightly constrained by tectonic fault boundaries (figure 2; electronic supplementary material, figures S1, S6, S7 and S9). Although Bayesian clustering methods detected admixture between populations at the fringe of the uplifted region, such admixture did not penetrate the core of the uplifted block. In contrast with the distinctive 'uplift' sectors detected for intertidal species, no such anomalies were detected for the co-distributed subtidal species, *D. willana* (figure 2; electronic supplementary material, figures S8 and S9). BAYESCAN tests detected only one uplift-associated outlier locus ($F_{ST} = 0.55$) in *D. antarctica* and none in *D. poha*. Population comparisons of *D. antarctica* within the uplift zone were characterized by particularly low F_{ST} values relative to most other pairwise comparisons (electronic supplementary material, figure S2).

Phylogenetic clustering of intertidal species using maximum likelihood (ML) and neighbour-joining confirmed the presence of shallow, yet unique evolutionary units confined to the uplifted zone for both species (figure 2; electronic

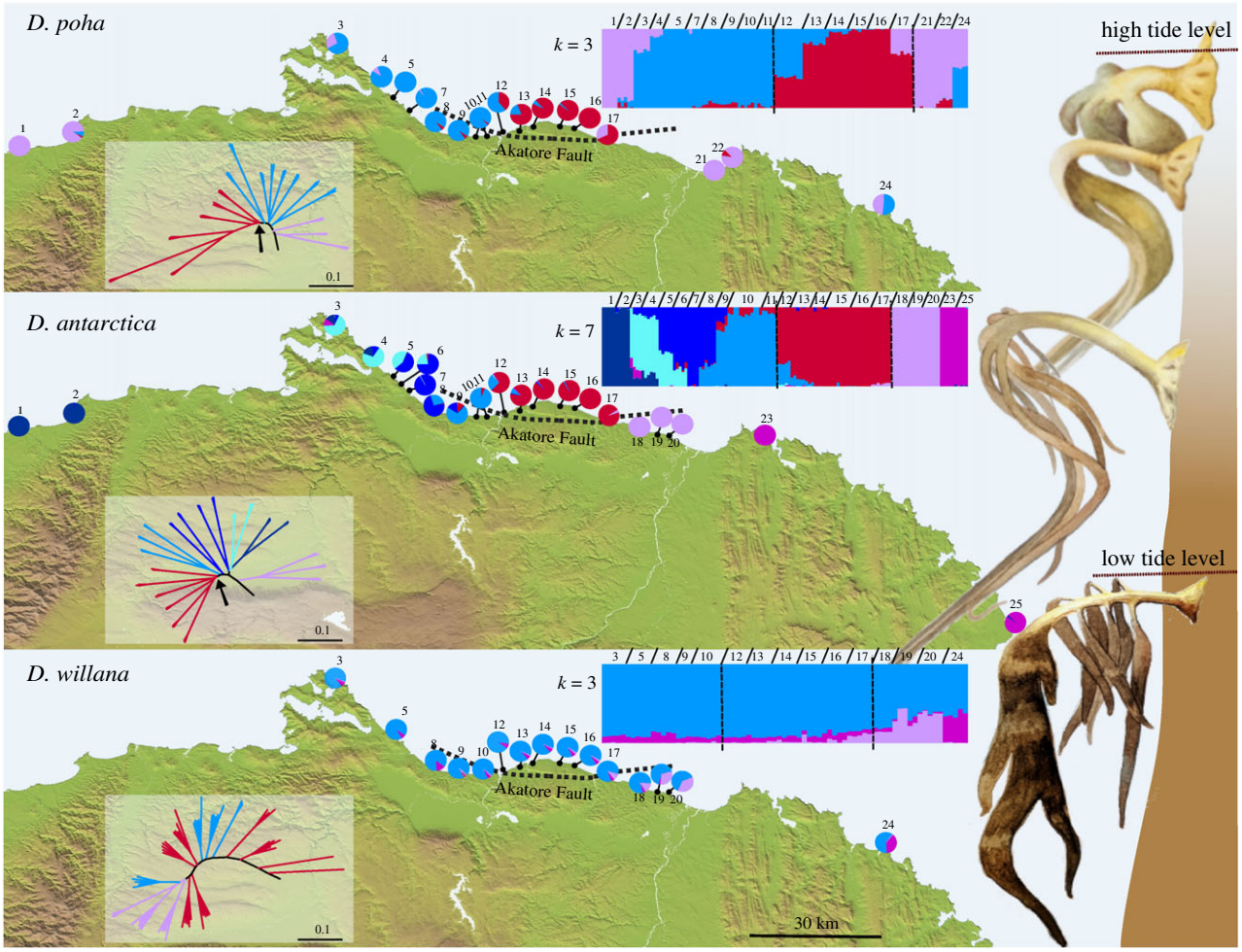

Figure 2. Evolution of distinctive genomic sectors (red) following recolonization of the uplifted Akatore coast. STRUCTURE plots of *D. poha* and *D. antarctica* reveal unique genotypic clusters tightly linked to the zone of coastal uplift. Neighbour-joining trees show the 'uplift' populations as separately evolving lineages (arrows) in both species. The co-distributed subtidal kelp, *D. willana*, does not show genomic evidence of response to the uplift disturbance presumably owing to its habitat choice. Pie charts represent admixture proportions per site. The uplifted Akatore coastal zone is indicated by dashed lines. Location codes are given in the electronic supplementary material, table S1. Kelp illustrations were retrieved from [28]. (Online version in colour.)

supplementary material, figure S1). By contrast, subtidal *D. willana* exhibited little phylogenetic differentiation among populations. Minor topological differences produced by different tree reconstruction methods, (figure 2 versus electronic supplementary material, figure S1) probably reflect the effects of genetic admixture at the edges of the uplift. Detailed descriptions of SNP-based population genomic statistics, population structure and phylogenetic results for each taxon are presented in the electronic supplementary material.

(b) Post-earthquake recolonization routes in intertidal kelps

Coalescent analyses of uplifted versus non-uplifted populations of *D. antarctica* and *D. poha* using DIYABC support the hypothesis that the uplift genomic 'sectors' evolved approximately 800 years ago at the time of the earthquake (figure 3). For *D. poha*, the demographic scenario with the highest posterior probability (median = 0.9969; 95% confidence interval (CI): 0.9961–0.9978) supported colonization of uplifted shores via admixture between northern and southern source populations. By contrast, *D. antarctica* is inferred to have reinvaded the uplifted zone from the north (median = 0.9626; 95% CI: 0.9542–0.971). In *D. poha*, colonization is estimated to have started 806 years ago (95% CI: 448–990), with expansion taking approximately 80 years (95% CI: 19.1–134.4), whereas in *D. antarctica* colonization probably started later (median = 876 year ago; 95% CI: 480–996), with expansion occurring within a few decades (median = 35.2 years; 95% CI: 8.2–105). The goodness of fit of the chosen scenario parameter-posterior combination was confirmed by checking the position of the observed dataset in the space of summary statistics (electronic supplementary material, figure S11). Posterior predictive errors using the direct approach implemented in DIYABC were 0.29 and 0.16 for *D. poha* and *D. antarctica*, respectively.

3. Discussion

(a) Tectonically generated biodiversity

Recent molecular studies have illustrated the importance of ancient geological processes in driving biological diversification over deep time scales [17,29,30]. Our study, by contrast, reveals the phylogeographic impacts of earthquake activity in driving spatial genomic shifts over ecologically relevant timeframes (e.g. within decades). Specifically, our finding that intertidal species with strong dispersal capacities show genetic discontinuities precisely matching earthquake uplift boundaries provides evidence of the potentially lasting genetic impacts of major geological disturbance.

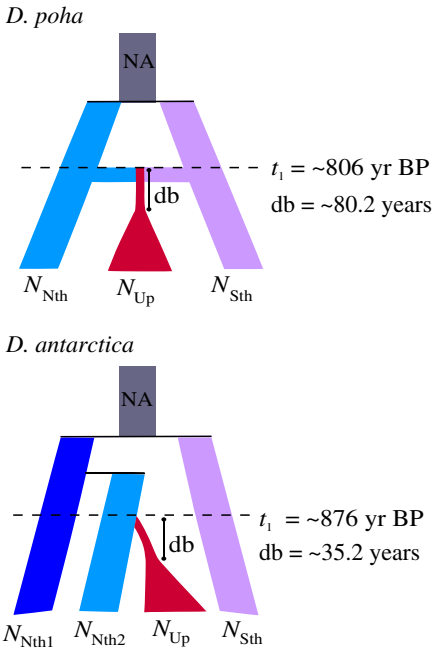

Figure 3. The most likely demographic models and estimated parameters from ABC analysis for *D. poha* and *D. antarctica* recolonization events. Populations recolonizing the uplifted Akatore coastal zone (N_{Up}) are indicated in red. t_1: timing of post-earthquake recolonization of intertidal habitats; db: bottleneck periods at the time of recolonization; *N*: effective populations size (see the electronic supplementary material, figure S10 for abbreviations and colour codes). (Online version in colour.)

SNP analyses indicate that rapid range expansion, coupled with apparent exclusion of late-dispersing genotypes, have interacted to facilitate parallel genotypic 'sweeps' into the uplifted zone for the two intertidal species (figure 2). Although the strong genetic distinction between uplifted and non-uplifted regions has been slightly 'blurred' at the margins via localized secondary admixture, the failure of such admixed genes to penetrate the centre of the uplift zone apparently highlights the 'founder takes all' (high-density blocking) dynamics [14,15] underpinning these rapid recolonization processes.

In contrast with clear genomic signatures of disruption in intertidal species, the absence of a population genomic signature of disruption in *D. willana* almost certainly reflects the subtidal (to 6 m) distribution of this species, which presumably allowed it to persist through the uplift event, as recently documented elsewhere in New Zealand [31]. Although the species probably suffered the considerable loss of abundance from the disturbance, with shallower individuals uplifted out of the water, even small refugial patches in the affected area could inhibit genomic turnover [16]. Additionally, the lack of buoyancy of this species makes it relatively unlikely to undergo long-distance dispersal via rafting and hence unlikely to evolve major genetic anomalies in response to such extirpation [13,16].

Although many studies assume that major genetic disjunctions within species reflect the action of natural selection and/or barriers to dispersal [32–34], our study highlights that the propagation of particular genotypes during range expansion can promote the evolution of large-scale spatial genetic structure over ecological time scales. Accordingly, recent demographic history can play a key role in explaining the distribution of spatial biodiversity and evolution in highly dynamic landscapes such as seismically active coastal areas [22,23,35].

(b) Rapid recolonization dynamics

Our demographic modelling supports the geologically derived hypothesis [26] that the Akatore Fault rupture event around 800 years ago caused widespread extirpation of intertidal kelps from the area (electronic supplementary material, table S8), consistent with direct observations of recent uplift events elsewhere [23,36]. *Durvillaea* kelps are habitat-forming species, hosting diverse epibiotic taxa, and thus their re-establishment can play an important role in post-disturbance recovery of southern rocky intertidal ecosystems [36]. Demographic modelling suggests that *D. poha* started to colonize the uplifted habitats earlier than *D. antarctica*, but took longer to expand its range than *D. antarctica* (figure 3; electronic supplementary material, table S8). The congeneric species investigated here have largely distinct habitat preferences (figure 2), and thus their recolonization dynamics are probably unaffected by one another. Minor differences in recolonization timing among these taxa might instead reflect the relatively fragmented distribution of sheltered *D. poha* habitats across the region, in contrast with continuous exposed *D. antarctica* habitats which probably promoted continuous and swift colonization of the latter species. The different temporal responses may also have been influenced by contrasting predation pressures experienced at early stages of recolonization [37] and the higher vulnerability of *D. poha* to heat stress [38].

The favoured demographic scenarios for both *D. antarctica* and *D. poha* indicate southward post-earthquake recolonization events, contrary to the prevailing northward oceanographic flow in this coastal region [39]. Such counter-current dispersals can be driven by strong storms and surface waves [40], which can override the effects of prevailing oceanographic features [40,41]. These findings also concur with those of a previous mtDNA phylogeographic analysis which similarly supported southward expansion of *D. antarctica* into this uplifted region [26]. Recolonization of *D. poha* probably involved a degree of admixture from both northern and southern source populations, perhaps facilitated by the relatively slow recolonization process inferred for populations of this ecologically relatively fragmented species.

(c) Genomic impacts of disturbance

Overall, our coastal uplift study highlights the potential impacts of ecosystem disturbance on the generation and distribution of intraspecific genetic diversity. These data reveal that disruptive earth-history events can simultaneously represent both destructive and creative forces for biological evolution [42]. Furthermore, disturbance outcomes can vary substantially among taxa, depending heavily on the habitat requirements and dispersal ability of focal species, as well the extent of habitat loss and mortality. This discovery of earthquake-generated, spatial genomic diversity on New Zealand shores has broader implications for the understanding and detection of major disturbance impacts in similarly dynamic landscapes worldwide (e.g. [22,43,44]). Moreover, as the scale of anthropogenic ecosystem disturbance events continues to accelerate [45,46], future multispecies genomic studies may be useful for detecting, understanding and mitigating the impacts of such upheaval.

4. Material and methods

(a) Sampling

The active Akatore Fault (figure 1*c*,*d*) is located in the southeast coast of New Zealand's South Island. Radiocarbon dating has

constrained the most recent fault rupture event to 600–900 years ago which has resulted in the uplift of 23 km of the coast by 2–4 m above the high-tide zone [25,26]. We applied a fine-scale sampling design (sampling every 2–6 km; taking into account non-habitable sandy shores. See the electronic supplementary material, table S1 for details), encompassing approximately 100 km of coastline, incorporating both the uplifted Akatore coast together with its flanking non-uplifted coastal regions. We collected samples of two intertidal kelp species, *D. poha* and *D. antarctica*. Vertical distribution and subsequent survival of these species depend on their exposure to surf [38]. Accordingly, and based on observations from the 2016 New Zealand Kaikoura earthquake [23], we hypothesized that uplifts higher than 2 m are enough to totally extirpate the intertidal populations. In addition, we considered a shallow subtidal species, *D. willana*, to control for the effect of the uplift on species with different vertical ranges. Collections were made during low tide in 2009, 2018 and 2019. Tissue samples were preserved in absolute ethanol in the field and further desiccated over silica gel beads at room temperature.

(b) Single nucleotide polymorphism analysis

DNA was extracted from desiccated samples using a PowerPlant Pro Kit and purified using a DNeasy PowerClean Pro Cleanup Kit (QIAGEN) with minor modifications as previously applied to bull kelps [24]. We used standard genotyping-by-sequencing (GBS) protocols [47] using the restriction enzyme PstI-HF (New England Biolabs). GBS libraries were created following the protocols previously used for *Durvillaea* [24]. Sequencing of the libraries in the 300–600 bp range was carried out on two lanes of a midoutput flowcell in an Illumina NextSeq 500 system (75 bp paired-end). We filtered out raw reads with an uncalled base and low-quality scores (PHRED score < 30) and demultiplexed combinatorial barcoded read pairs using the *process_radtags* algorithm implemented in Stacks 2 [48]. We truncated the final reads to 68 bp and used them to assemble loci *de novo* using Stacks. We optimized Stacks parameters for each species separately using guidelines described in [49] (electronic supplementary material, table S2). We only retained biallelic loci that were present in at least 50% of the sampling sites and 80% of individuals from each sampling site. We removed potential paralogous loci by increasing the maximum observed heterozygosity cut-off to 0.7. In order to understand how population genomic inferences might be affected by the maximum observed heterozygosity threshold and highly correlated loci, we generated three more SNP datasets for population structure analysis. Details on the comparison of these datasets with our main SNP dataset are presented in the electronic supplementary material.

(c) Statistical approach

We used Stacks to calculate population genomic statistics including F_{IS} (inbreeding coefficent), π (overall population genetic diversity index), observed and expected heterozygosity and homozygosity. We used the R package StAMPP 1.5.1 [50] to calculate pairwise F_{ST} using 100 bootstraps.

To assess population structure, we ran a PCA [51,52], Structure 2.3.4 [53] and BAPS 6.0 [54] on all sampling sites of each species. For all Structure analyses we used default parameter settings, 500 000 iterations, 50 000 burn-in steps and 10 replicates for each potential *K*. For all BAPS analyses, we first ran individual level mixture analysis with 10 replicates for each *K* and then used the mixture results to infer admixture coefficients with 1000 iterations. For both Bayesian clustering methods, we only used the first SNP per locus to remove correlated SNPs within each locus, excluded sampling site information and analysed $K = 2$–10 clusters. To choose the optimal K for Structure analyses, we used the delta *K* method [55]. All plots were visualized using pophelper [56]. To infer phylogenetic relationships between different populations, we constructed unrooted ML and neighbour-joining trees using IQtree 1.6.12 [57] and VCF-kit 0.1.6 [58], respectively. For all population tree constructions of *D. antarctica* and *D. poha*, we randomly chose three samples from each studied population and included published sequences from elsewhere in the New Zealand region [24] to determine broad-scale phylogeographic structure (electronic supplementary material, table S4). ML analyses were performed using 5000 ultrafast bootstrap replicates and the ModelFinder algorithm implemented in IQtree.

To test the presence of outlier loci, we used Bayescan 2.1 [59]. We carried out the test on uplifted versus non-uplifted categories based on Structure and BAPS results. We used default chain parameters and 100 prior odds for the neutral model to minimize false-positive rates.

To evaluate the best post-earthquake recolonization routes in intertidal species, we used an approximate Bayesian computation approach in DIYABC 2.1.0 [60]. We grouped samples based on the clustering results (electronic supplementary material, table S5) and restricted the maximum number of missing data in the DIYABC input SNP dataset to 14 for *D. antarctica* and 12 in *D. poha*. With this approach, we minimized the missing data while maintaining the population structure patterns similar to their corresponding full datasets. We formulated four demographic scenarios for *D. antarctica* and three demographic scenarios for *D. poha* to identify the most probable recolonization route into the uplifted coasts (see the electronic supplementary material, Appendix for details). All scenarios were characterized by a bottleneck period starting at the time of the earthquake (see the electronic supplementary material, table S6 for the details of priors used). We simulated one million summary statistics (SuSt; electronic supplementary material, table S7) per scenario and initially evaluated potential misspecifications in our scenarios and prior distributions of parameters using a PCA. We then used the logistic approach on 1% of the closest simulated SuSt to the observed SuSt to calculate the posterior probability of the scenarios. The goodness-of-fit of models with the highest posterior probabilities was evaluated using the model checking option in DIYABC. We also calculated posterior based error by simulating 1000 pseudo-observed datasets under each competing scenario and computing scenarios probabilities by choosing the direct estimate based on 500 datasets closest to the observed datasets. After choosing the most probable scenario, we used the 1% closest simulated data to estimate the parameters of the model (electronic supplementary material, table S8).

Data accessibility. Raw demultiplexed reads are available on the NCBI Sequence Read Archive under project ID. PRJNA635712. SNP data, metadata, ABC input and scenario files are available at Dryad Digital repository: https://dx.doi.org/10.5061/dryad.pg4f4qrkm [61].

Authors' contributions. E.P., C.I.F. D.C. and J.M.W. designed research. E.P. generated data. E.P. and L.D. analysed data. E.P. wrote the paper. All authors edited the paper.

Competing interests. We declare we have no competing interests.

Funding. This study was supported by the Marsden Fund administered by Royal Society of New Zealand (UOO1818) awarded to J.M.W., Rutherford Fellowship grant (UOO1803) awarded to C.I.F. and an Otago PhD Scholarship awarded to E.P. LIDAR data were supplied by Otago Regional Council and constructed into a topographic map by Dr Stephen Read.

Acknowledgement. We thank Dr Tania King for substantial help with laboratory procedures, and Pamela Olmedo Rojas and Felix Vaux for assisting us with fieldwork. We wish to acknowledge the use of New Zealand eScience Infrastructure (NeSI) high-performance computing facilities as part of this research.

References

1. Hewitt G. 2000 The genetic legacy of the Quaternary ice ages. *Nature* **405**, 907–913. (doi:10.1038/35016000)
2. Chen IC, Hill JK, Ohlemüller R, Roy DB, Thomas CD. 2011 Rapid range shifts of species associated with high levels of climate warming. *Science* **333**, 1024–1026. (doi:10.1126/science.1206432)
3. Gaston KJ. 2000 Global patterns in biodiversity. *Nature* **405**, 220–227. (doi:10.1038/35012228)
4. Hallatschek O, Hersen P, Ramanathan S, Nelson DR. 2007 Genetic drift at expanding frontiers promotes gene segregation. *Proc. Natl Acad. Sci. USA* **104**, 19 926–19 930. (doi:10.1073/pnas.0710150104)
5. Excoffier L, Ray N. 2008 Surfing during population expansions promotes genetic revolutions and structuration. *Trends Ecol. Evol.* **23**, 347–351. (doi:10.1016/j.tree.2008.04.004)
6. de Aguiar MAM, Baranger M, Baptestini EM, Kaufman L, Bar-Yam Y. 2009 Global patterns of speciation and diversity. *Nature* **460**, 384–387. (doi:10.1038/nature08168)
7. Excoffier L, Foll M, Petit RJ. 2009 Genetic consequences of range expansions. *Annu. Rev. Ecol. Evol. Syst.* **40**, 481–501. (doi:10.1146/annurev.ecolsys.39.110707.173414)
8. Hallatschek O, Nelson DR. 2010 Life at the front of an expanding population. *Evolution* **64**, 193–206. (doi:10.1111/j.1558-5646.2009.00809.x)
9. Momigliano P, Jokinen H, Fraimout A, Florin A-B, Norkko A, Merilä J. 2017 Extraordinarily rapid speciation in a marine fish. *Proc. Natl Acad. Sci. USA* **114**, 6074–6079. (doi:10.1073/pnas.1615109114)
10. Hubbell SP. 2001 *The unified neutral theory of biodiversity and biogeography*. Princeton, NJ: Princeton University Press.
11. Edmonds CA, Lillie AS, Cavalli-Sforza LL. 2004 Mutations arising in the wave front of an expanding population. *Proc. Natl Acad. Sci. USA* **101**, 975–979. (doi:10.1073/pnas.0308064100)
12. Klopfstein S, Currat M, Excoffier L. 2006 The fate of mutations surfing on the wave of a range expansion. *Mol. Biol. Evol.* **23**, 482–490. (doi:10.1093/molbev/msj057)
13. Ibrahim KM, Nichols RA, Hewitt GM. 1996 Spatial patterns of genetic variation generated by different forms of dispersal during range expansion. *Heredity* **77**, 282–291. (doi:10.1038/hdy.1996.142)
14. Waters JM, Fraser CI, Hewitt GM. 2013 Founder takes all: density-dependent processes structure biodiversity. *Trends Ecol. Evol.* **28**, 78–85. (doi:10.1016/j.tree.2012.08.024)
15. De Meester L, Vanoverbeke J, Kilsdonk LJ, Urban MC. 2016 Evolving perspectives on monopolization and priority effects. *Trends Ecol. Evol.* **31**, 136–146. (doi:10.1016/j.tree.2015.12.009)
16. Fraser CI, Davies ID, Bryant D, Waters JM. 2018 How disturbance and dispersal influence intraspecific structure. *J. Ecol.* **106**, 1298–1306. (doi:10.1111/1365-2745.12900)
17. Beheregaray LB, Ciofi C, Geist D, Gibbs JP, Caccone A, Powell JR. 2003 Genes record a prehistoric volcano eruption in the Galápagos. *Science* **302**, 75. (doi:10.1126/science.1087486)
18. Hung KH, Hsu TW, Schaal BA, Chiang TY. 2005 Loss of genetic diversity and erroneous phylogeographical inferences in *Lithocarpus konishii* (Fagaceae) of Taiwan caused by the Chi-Chi earthquake: implications for conservation. *Ann. Mo. Bot. Gard.* **92**, 52–65.
19. Kume M, Mori S, Kitano J, Sumi T, Nishida S. 2018 Impact of the huge 2011 Tohoku-oki tsunami on the phenotypes and genotypes of Japanese coastal threespine stickleback populations. *Sci. Rep.* **8**, 1–11. (doi:10.1038/s41598-018-20075-z)
20. Farías M, Vargas G, Tassara A, Carretier S, Baize S, Melnick D, Bataille K. 2010 Land-level changes produced by the Mw 8.8 2010 Chilean earthquake. *Science* **329**, 916. (doi:10.1126/science.1192094)
21. Ruiz S *et al*. 2016 The seismic sequence of the 16 September 2015 Mw 8.3 Illapel, Chile, Earthquake. *Seismol. Res. Lett.* **87**, 789–799. (doi:10.1785/0220150281)
22. Jaramillo E, Dugan JE, Hubbard DM, Melnick D, Manzano M, Duarte C, Campos C, Sanchez R. 2012 Ecological implications of extreme events: footprints of the 2010 earthquake along the Chilean coast. *PLoS ONE* **7**, e35348. (doi:10.1371/journal.pone.0035348)
23. Hamling IJ *et al*. 2017 Complex multifault rupture during the 2016 Mw 7.8 Kaikōura earthquake, New Zealand. *Science* **356**, aam7194. (doi:10.1126/science.aam7194)
24. Peters JC, Waters JM, Dutoit L, Fraser CI. 2020 SNP analyses reveal a diverse pool of potential colonists to earthquake-uplifted coastlines. *Mol. Ecol.* **29**, 149–159. (doi:10.1111/mec.15303)
25. Litchfield NJ, Lian OB. 2004 Luminescence age estimates of Pleistocene marine terrace and alluvial fan sediments associated with tectonic activity along coastal Otago, New Zealand. *N. Z. J. Geol. Geophys.* **47**, 29–37. (doi:10.1080/00288306.2004.9515035)
26. Parvizi E, Craw D, Waters JM. 2019 Kelp DNA records late Holocene paleoseismic uplift of coastline, southeastern New Zealand. *Earth Planet. Sci. Lett.* **520**, 18–25. (doi:10.1016/j.epsl.2019.05.034)
27. Taylor-Silva BI, Stirling MW, Litchfield NJ, Griffin JD, van den Berg EJ, Wang N. 2020 Paleoseismology of the Akatore Fault, Otago, New Zealand. *N. Z. J. Geol. Geophys*. **63**, 151–167. (doi:10.1080/00288306.2019.1645706)
28. Fraser CI, Velásquez M, Nelson WA, Macaya EC, Hay CH. 2020 The biogeographic importance of buoyancy in macroalgae: a case study of the southern bull-kelp genus *Durvillaea* (Phaeophyceae), including descriptions of two new species. *J. Phycol.* **56**, 23–36. (doi:10.1111/jpy.12939)
29. Riddle BR, Hafner DJ, Alexander LF, Jaeger JR. 2000 Cryptic vicariance in the historical assembly of a Baja California Peninsular Desert biota. *Proc. Natl Acad. Sci. USA* **97**, 14 438–14 443. (doi:10.1073/pnas.250413397)
30. Craw D, Upton P, Burridge CP, Wallis GP, Waters JM. 2016 Rapid biological speciation driven by tectonic evolution in New Zealand. *Nat. Geosci.* **9**, 140–144. (doi:10.1038/ngeo2618)
31. Thomsen MS, Metcalfe I, Siciliano A, South PM, Gerrity S, Alestra T, Schiel DR. 2020 Earthquake-driven destruction of an intertidal habitat cascade. *Aquat. Bot.* **164**, 103217. (doi:10.1016/j.aquabot.2020.103217)
32. Korol A, Rashkovetsky E, Iliadi K, Michalak P, Ronin Y, Nevo E. 2000 Nonrandom mating in *Drosophila melanogaster* laboratory populations derived from closely adjacent ecologically contrasting slopes at 'Evolution Canyon'. *Proc. Natl Acad. Sci. USA* **97**, 12 637–12 642. (doi:10.1073/pnas.220041397)
33. Hendry AP, Nosil P, Rieseberg LH. 2007 The speed of ecological speciation. *Funct. Ecol.* **21**, 455–464. (doi:10.1111/j.1365-2435.2007.01240.x)
34. Smith BT *et al*. 2014 The drivers of tropical speciation. *Nature* **515**, 406–409. (doi:10.1038/nature13687)
35. Plafker G, Savage JC. 1970 Mechanism of the Chilean earthquakes of May 21 and 22, 1960. *GSA Bull.* **81**, 1001–1030. (doi:10.1130/0016-7606(1970)81[1001:MOTCEO]2.0.CO;2)
36. Schiel DR *et al*. 2019 The Kaikōura earthquake in southern New Zealand: loss of connectivity of marine communities and the necessity of a cross-ecosystem perspective. *Aquat. Conserv. Mar. Freshw. Ecosyst.* **29**, 1520–1534. (doi:10.1002/aqc.3122)
37. Taylor DI, Schiel DR. 2010 Algal populations controlled by fish herbivory across a wave exposure gradient on southern temperate shores. *Ecology* **91**, 201–211. (doi:10.1890/08-1512.1)
38. Thomsen MS, Mondardini L, Alestra T, Gerrity S, Tait L, South PM, Lilley SA, Schiel DR. 2019 Local extinction of bull kelp (*Durvillaea* spp.) due to a marine heatwave. *Front. Mar. Sci.* **6**, 84. (doi:10.3389/fmars.2019.00084)
39. Chiswell SM. 2009 Colonisation and connectivity by intertidal limpets among New Zealand, Chatham and Sub-Antarctic Islands. II. Oceanographic connections. *Mar. Ecol. Prog. Ser.* **388**, 121–135. (doi:10.3354/meps08167)
40. Fraser CI *et al*. 2018 Antarctica's ecological isolation will be broken by storm-driven dispersal and warming. *Nat. Clim. Change* **8**, 704–708. (doi:10.1038/s41558-018-0209-7)
41. Waters JM, King TM, Fraser CI, Craw D. 2018 Crossing the front: contrasting storm-forced dispersal dynamics revealed by biological, geological and genetic analysis of beach-cast kelp. *J. R. Soc. Interface* **15**, 20180046. (doi:10.1098/rsif.2018.0046)

42. Wallis GP, Waters JM, Upton P, Craw D. 2016 Transverse alpine speciation driven by glaciation. *Trends Ecol. Evol.* **31**, 916–926. (doi:10.1016/j.tree.2016.08.009)
43. Thom D, Seidl R. 2016 Natural disturbance impacts on ecosystem services and biodiversity in temperate and boreal forests. *Biol. Rev.* **91**, 760–781. (doi:10.1111/brv.12193)
44. Kanamori Y, Iwasaki A, Oda S, Noda T. 2020 Interspecific differences in the recovery of rocky intertidal zonation after the 2011 Great East Japan Earthquake. *Ecol. Res.* **35**, 95–105. (doi:10.1111/1440-1703.12085)
45. Fischer J, Lindenmayer DB. 2007 Landscape modification and habitat fragmentation: a synthesis. *Glob. Ecol. Biogeogr.* **16**, 265–280. (doi:10.1111/j.1466-8238.2007.00287.x)
46. Pickrell J. 2019 Australian blazes will 'reframe our understanding of bushfire'. *Science* **366**, 937. (doi:10.1126/science.366.6468.937)
47. Elshire RJ, Glaubitz JC, Sun Q, Poland JA, Kawamoto K, Buckler ES, Mitchell SE. 2011 A robust, simple genotyping-by-sequencing (GBS) approach for high diversity species. *PLoS ONE* **6**, e19379. (doi:10.1371/journal.pone.0019379)
48. Rochette NC, Rivera-Colón AG, Catchen JM. 2019 Stacks 2: Analytical methods for paired-end sequencing improve RADseq-based population genomics. *Mol. Ecol.* **28**, 4737–4754. (doi:10.1111/mec.15253)
49. Paris JR, Stevens JR, Catchen JM. 2017 Lost in parameter space: a road map for stacks. *Methods Ecol. Evol.* **8**, 1360–1373. (doi:10.1111/2041-210X.12775)
50. Pembleton LW, Cogan NOI, Forster JW. 2013 StAMPP: an R package for calculation of genetic differentiation and structure of mixed-ploidy level populations. *Mol. Ecol. Resour.* **13**, 946–952. (doi:10.1111/1755-0998.12129)
51. Patterson N, Price AL, Reich D. 2006 Population structure and eigenanalysis. *PLoS Genet.* **2**, e190. (doi:10.1371/journal.pgen.0020190)
52. Jombart T. 2008 adegenet: a R package for the multivariate analysis of genetic markers. *Bioinformatics* **24**, 1403–1405. (doi:10.1093/bioinformatics/btn129)
53. Pritchard JK, Stephens M, Donnelly P. 2000 Inference of population structure using multilocus genotype data. *Genetics* **155**, 945–959.
54. Corander J, Marttinen P, Sirén J, Tang J. 2008 Enhanced Bayesian modelling in BAPS software for learning genetic structures of populations. *BMC Bioinf.* **9**, 539. (doi:10.1186/1471-2105-9-539)
55. Evanno G, Regnaut S, Goudet J. 2005 Detecting the number of clusters of individuals using the software STRUCTURE: a simulation study. *Mol. Ecol.* **14**, 2611–2620. (doi:10.1111/j.1365-294X.2005.02553.x)
56. Francis RM. 2017 pophelper: an R package and web app to analyse and visualize population structure. *Mol. Ecol. Resour.* **17**, 27–32. (doi:10.1111/1755-0998.12509)
57. Nguyen LT, Schmidt HA, von Haeseler A, Minh BQ. 2015 IQ-TREE: a fast and effective stochastic algorithm for estimating maximum-likelihood phylogenies. *Mol. Biol. Evol.* **32**, 268–274. (doi:10.1093/molbev/msu300)
58. Cook DE, Andersen EC. 2017 VCF-kit: assorted utilities for the variant call format. *Bioinformatics* **33**, 1581–1582. (doi:10.1093/bioinformatics/btx011)
59. Foll M, Gaggiotti O. 2008 A genome-scan method to identify selected loci appropriate for both dominant and codominant markers: a Bayesian perspective. *Genetics* **180**, 977–993. (doi:10.1534/genetics.108.092221)
60. Cornuet JM, Pudlo P, Veyssier J, Dehne-Garcia A, Gautier M, Leblois R, Marin JM, Estoup A. 2014 DIYABC v2.0: a software to make approximate Bayesian computation inferences about population history using single nucleotide polymorphism, DNA sequence and microsatellite data. *Bioinformatics* **30**, 1187–1189. (doi:10.1093/bioinformatics/btt763)
61. Parvizi E, Fraser CI, Dutoit L, Craw D, Waters JM. 2020 Data from: The genomic footprint of coastal earthquake uplift. Dryad Digital Repository. (https://doi.org/10.5061/dryad.pg4f4qrkm)